C. R. Mecanique 341 (2013) 469–476

Contents lists available at SciVerse ScienceDirect

Comptes Rendus Mecanique

www.sciencedirect.com

10th International Meeting on Thermodiffusion

# Molecular dynamics simulation of thermodiffusion and mass diffusion in structureless and atomistic micropores

Rachid Hannaoui, Guillaume Galliéro *, Christian Boned

*LFC-R (UMR5150 with CNRS and Total), Université de Pau et des Pays de l'Adour, BP 1151, 64013 Pau Cedex, France*

ARTICLE INFO

*Article history:*
Available online 28 February 2013

*Keywords:*
Lennard–Jones
Mass diffusion
Molecular dynamics
Porous medium
Thermodiffusion
Soret effect

ABSTRACT

In this work, we have studied the effect of surface roughness on thermodiffusion in simple "isotopic" mixtures confined in a slit nanopore. To do so, we have performed non-equilibrium molecular dynamics simulations of Lennard–Jones binary equimolar mixtures confined in structureless (in which the interaction with the fluid is described by a Lennard–Jones 9–3 potential) and atomistic walls for various widths, from 5 to 35 times the size of a molecule, in the $NP_{//}T$ ensemble. For that purpose, a new algorithm is proposed in atomistic pore. Different super-critical conditions have been explored, ranging from low to moderate densities. In addition to the thermal diffusion factor, we have also estimated the mass diffusion and thermodiffusion coefficients separately. The results show that the two types of walls lead to noticeably different results. The thermal diffusion factor tends to increase in atomistic wall and slightly decrease in structureless wall when the pore width is decreasing, this being related to the average density behaviour. More precisely, both mass and thermodiffusion coefficients are weakly affected by the pore width for structureless walls, whereas both quantities largely decrease (up to 70% and 55% respectively compared to bulk fluid) when pore size decreases in the case of a rough solid surface because of the friction on the walls.



## 1. Introduction

A temperature gradient in a multi-component mixture can induce a relative species migration, due to the phenomenon known as Soret effect or thermodiffusion [1]. This phenomenon plays a crucial role in many natural processes and industrial applications such as the vertical spatial variation of the composition in petroleum reservoirs before production [2–4].

It is generally assumed that the porous medium, through tortuosity, has a similar influence on the mass and thermodiffusion coefficients [5,6], i.e. the thermal diffusion factor (or equivalently the Soret coefficient) is not affected by the presence of a porous medium. However, in very low permeability porous medium (in which the pore widths are of the order of a few molecular diameters), the behaviour of the confined fluid is considerably different from the behaviour of the corresponding bulk fluid [7]. In particular, we can mention the strong inhomogeneity of the confined fluid due to adsorption and molecular packing effects [7]. In the past, some works have been carried out to determine the porous medium effect on thermodiffusion by using molecular dynamics simulation [8–12], but the analysis was not always easy to handle because of the impossibility to get rid of the selective adsorption [8–11].

To simplify the analysis of the influence of the size of a porous medium on thermodiffusion, we have used "isotope" binary mixtures. In these mixtures, both compounds have the same interaction parameters (size and energy), but different

* Corresponding author.
*E-mail address:* guillaume.galliero@univ-pau.fr (G. Galliéro).

1631-0721/$ – see front matter 
http://dx.doi.org/10.1016/j.crme.2013.01.015

masses. So the two components are completely equivalent in terms of adsorption and thermodynamic properties, which allows focusing only on the porous medium effect (confinement + molecular packing) on the thermodiffusion. Following a previous work dedicated to structureless slit pore only [13], we have tried in this work to quantify the impact of the roughness of the solid surface on the results as it is known that this parameter has an impact on mass diffusion [7,14]. To do so, using the same ensemble ($NP_{//}T$) we have compared the atomistic and structureless walls effect on thermodiffusion. More precisely, we have performed a systematic study of the influence of pore widths varying from 5 to 35 times of molecular diameter, at four different parallel pressures in a super-critical state, for two descriptions of the wall, one based on an integrated potential (structureless) and another one based on an atomistic description of the walls.

## 2. Theory & model

### 2.1. Fluid description

In this work, the fluid particles are described by smooth spheres, interacting through a truncated 12–6 Lennard–Jones potential:

$$U(r_{ij}) = 4\varepsilon\left[\left(\frac{\sigma}{r_{ij}}\right)^{12} - \left(\frac{\sigma}{r_{ij}}\right)^{6}\right] \tag{1}$$

where $\varepsilon_{ij}$ and $\sigma_{ij}$ represent respectively the intermolecular potential depth and the molecular diameter, $r_{ij}$ is the distance between particle $i$ and particle $j$. To perform the computation, the potential is truncated at a cut-off radius $r_c = 3.5\sigma$. Furthermore, long-range corrections are derived from the Wang and Fichthorn formulation [15], which are based on a classical approximation of a radial distribution function equal to one for a distance above the cut-off radius and can be used to deal with confined systems. The equations of motion are integrated using the "velocity Verlet" algorithm [16]. To save CPU time, we have used the Verlet neighbour list [16]. In the following, LJ reduced quantities are expressed with a star as superscript [13].

As mentioned in the introduction, to focus only on the confinement effect on thermodiffusion, we have used "isotopic" binary mixtures in which the two compounds have the same interaction parameters ($\varepsilon$ and $\sigma$) but different masses ($m_2 = 10m_1$).

### 2.2. Solid phase description

In this work the solid was modelled by two parallel planes placed in $z$-direction and separated by a given reduced distance $H* = H/\sigma$. This distance corresponds to the distance between the positions of the two solids where the potential is infinite. We have used two types of walls, as shown on Fig. 1. The first wall model is an integrated wall which is structureless. In that model the Lennard–Jones 9–3 potential has been used (without truncation) to describe the fluid–solid interactions:

$$U(d) = 4\pi\varepsilon\left[\frac{1}{45}\left(\frac{\sigma}{d}\right)^{9} - \frac{1}{6}\left(\frac{\sigma}{d}\right)^{3}\right] \tag{2}$$

where $d$ is the distance between the particle and one wall, $\varepsilon$ and $\sigma$ the solid–fluid molecular parameters taken equal to those of the fluid.

The second wall model is an atomistic wall, modelled as harmonic faced centred cubic crystal with a density equal to the one employed for the integrated wall model. The interaction has been truncated at a distance equal to fluid–fluid interaction. This representation of the wall is more realistic, but is more time consuming. However, it allows us to avoid some artefacts such as thermal creep (microscopic Marangoni effect) in the simulation box [8,11]. Indeed, when changing a flat wall into a slightly corrugated wall, it is shown that the dynamic behaviour of confined fluids can be drastically modified, while the average static properties are not affected [7].

As an example the stationary state of the local fluid density for different wall types and of the same isotopic mixture in the $z$-direction is shown in Fig. 2. As expected, a strong inhomogeneity perpendicular to the walls ($z$-direction) can be observed, induced by adsorption and molecular packing.

When comparing the two wall types' results, the fluid molecules are, especially for the lowest pressure state (see Fig. 2(a)) noticeably more attracted by the atomistic walls than by the structureless walls. This difference leads to non-negligible differences, even in the central part of the pore in the less dense cases, and confirms that the integrated potential provided by Eq. (2) is unable to correctly mimic the potential associated with an atomistic description of the walls [7]. However, these differences are reduced when increasing the pressure and enlarging the pore width, see Fig. 2(b), with a density in the central part of the pore that is almost the same for the two wall types and is equal to the bulk density (bulk values correspond to the results in the absence of walls).

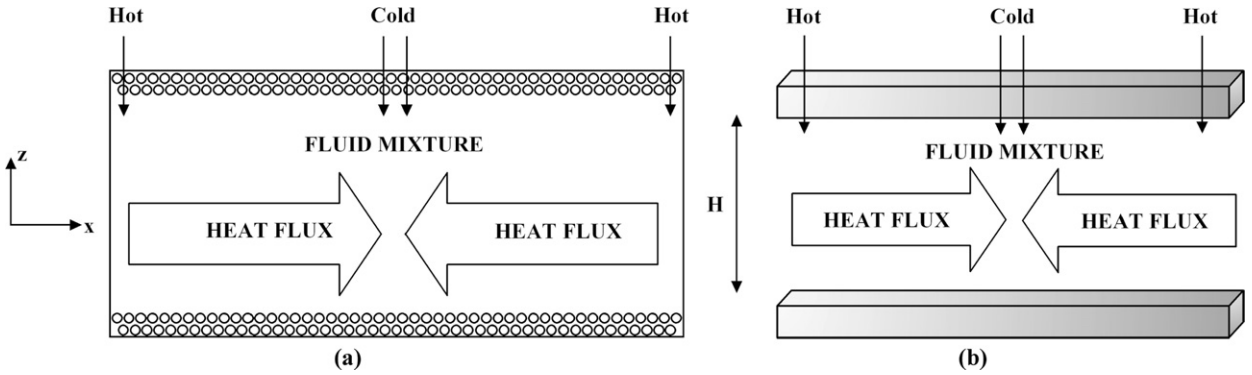


**Fig. 1.** General scheme of the system used in the NEMD simulations for different type of walls: atomistic wall (a) and integrated wall (b).

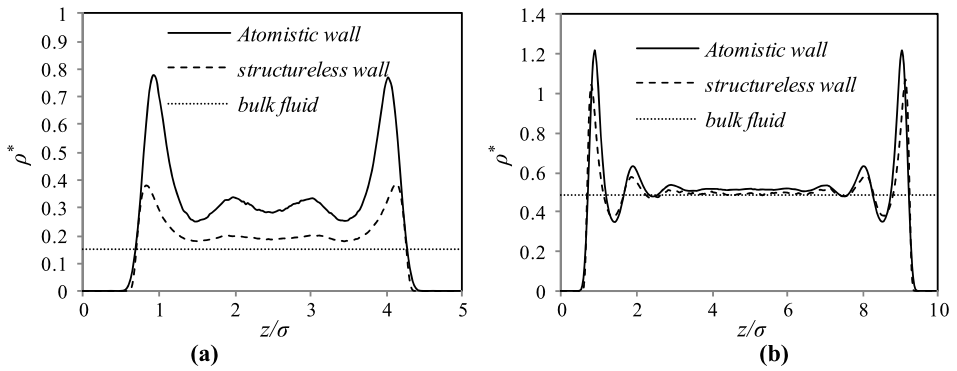


**Fig. 2.** Reduced local density of the fluid confined in pore at $T^* = 2$ for (a) $H^* = 5$ and $P^*_{//} = 0.25$, (b) $H^* = 10$ and $P^*_{//} = 1$. Dotted line corresponds to the bulk density.

### 2.3. $NP_{//}T$ ensemble

To study diffusion/thermodiffusion of confined fluids using molecular simulation methods for various pore widths, the simulation should be done in a grand canonical ensemble, in which chemical potential, volume, and temperature are constant. However, these methods are not easy to implement in molecular dynamics simulations. Recently, Wang and Fichthorn [15] have proposed an alternative to this ensemble, the so-called $NP_{//}T$ ensemble, where $N$ is the number of particles, $T$ is the average temperature, and $P_{//}$ is the parallel (to the walls) component of the pressure/stress, in which they used the Evans and Morriss barostat [16]. Eslami and Müller-Plathe [17] have proposed another algorithm, in which they have used a Berendsen barostat [18] to control the parallel pressure by changing the pore width. It has been shown that such an ensemble gives similar results to that of a true Grand Canonical one, even if not being fully equivalent [17].

It is rather easy to impose a given $P_{//}$ when using integrated walls (by changing the simulation box size in $x$- or $y$-direction); however, when dealing with atomistic walls, if the pore width is kept constant, there exists no alternative published in the literature. So, for this purpose, we have developed an algorithm to control the parallel pressure of a fluid confined between atomistic walls for a fixed pore width. Here we briefly describe the steps of our $NP_{//}T$ ensemble Molecular Dynamics simulation:

(1) Impose the density step $\Delta\rho$, the desired parallel pressure $P^{\mathrm{d}}_{//}$, a tolerance parameter $\delta$ and an initial density $\rho$.
(2) Generate an initial configuration (positions, velocities and accelerations).
(3) Make a simulation in the $NVT$ ensemble (where $V$ is the volume) during $n$ time-steps (typically, $n = 10^4$); here the Berendsen thermostat has been used [18].
(4) Evaluate the average parallel pressure $P^{\mathrm{new}}_{//}$.
(5) If $|P^{\mathrm{new}}_{//} - P^{\mathrm{d}}_{//}| \leqslant \delta$, then end.
(6) If the parallel pressure is between previous and new parallel pressures the density step, $\Delta\rho$ is divided by 2.
(7) If $P^{\mathrm{new}}_{//} < P^{\mathrm{d}}_{//}$, then $\rho^{\mathrm{new}} = \rho + \Delta\rho$ and if $P^{\mathrm{new}}_{//} > P^{\mathrm{d}}_{//}$, then $\rho^{\mathrm{new}} = \rho - \Delta\rho$.
(8) Generate a system with the new density $\rho^{\mathrm{new}}$ and go back to step number 2.

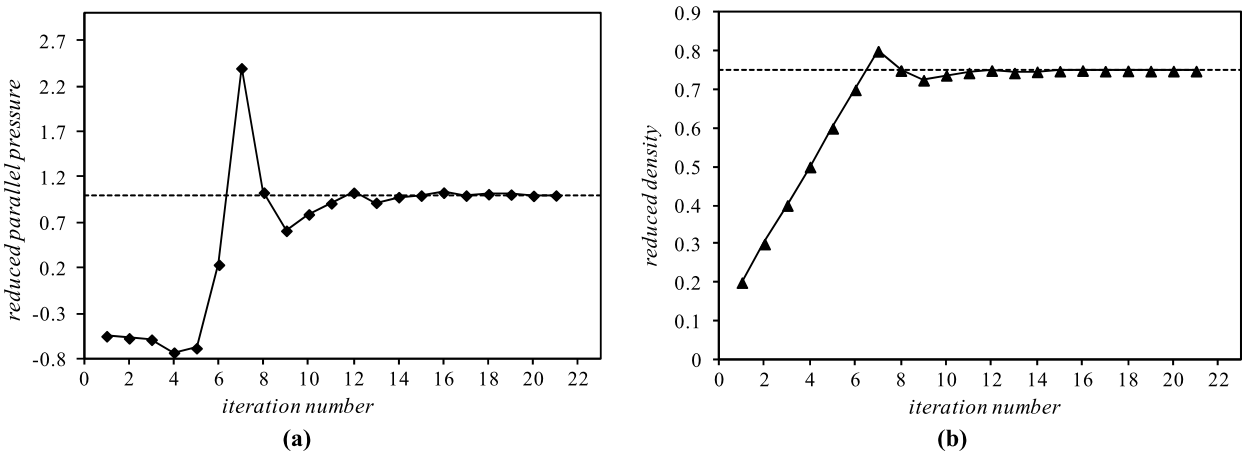


**Fig. 3.** Evolution of the parallel pressure (a) and average density (b) as a function of the iteration number.

To test our algorithm, the simulation has been performed for sub-critical conditions ($T^* = 1$) in a pore width of $5\sigma$ with a target parallel pressure equal to 1 (see Fig. 3). Initial conditions are $\rho^* = 0.2$ and $\Delta\rho^* = 0.1$. Fig. 3 shows that the system is already close to the desired parallel pressure in 10 iterations, despite an initial system far from the final state, which means that the algorithm converges. Furthermore, as expected, the density has a similar behaviour with less pronounced fluctuations

### 2.4. Computed quantities

After having imposed the parallel pressure for a given pore width we have performed simulations using a non-equilibrium molecular dynamics (NEMD) scheme proposed in [19] for $1.5 \times 10^7$ time-steps to ensure a sufficient statistical averaging. At the stationary state, the thermal diffusion factor has been computed using:

$$\alpha_T = -\frac{T}{x(1-x)}\frac{\nabla x}{\nabla T} \tag{3}$$

where $x$ is the molar fraction of the heaviest compound (i.e. species 2 in this work) and $T$ the temperature. Concerning the mass diffusion, $D$, we have used the classical mean square displacement of both species [11] over the two directions parallel to the walls to compute the two self diffusion coefficients $D_1$ and $D_2$. Then we have used the fact that the mixture studied is ideal, which allows us to employ the following relation [13]:

$$D = x_1 D_2 + x_2 D_1 \tag{4}$$

Finally, the thermodiffusion coefficient, $D_T$, is deduced from the thermal diffusion factor and the mass diffusion coefficient using:

$$D_T = D\frac{\alpha_T}{T} \tag{5}$$

Error bars have been computed using the classical sub-blocks method [16]. They have not been included in Figs. 4–7 for the sake of clarity, but they are of the order of 1% for density and mass diffusion and smaller than 15% for the thermodiffusion factor.

## 3. Results and discussion

### 3.1. Density

As mentioned previously, we have studied a simple equimolar "isotopic" binary mixture confined between atomistic and structureless walls. The pore width varies between 5 to 35 times of a size molecule. We have studied the effect of the parallel pressure using $P^*_{//} = 0.25$, 0.5, 0.75 and 1, corresponding to a bulk density of $0.148 \pm 0.01$, $0.306 \pm 0.03$, $0.416 \pm 0.04$ and $0.483 \pm 0.05$, respectively. To avoid phase transitions, we have performed our simulations at a super-critical temperature ($T^* = 2$). In addition, it should be mentioned that the average densities so obtained have been estimated over the full pore space (i.e. over $H^*$) even if there is no fluid present very close to the walls, see Fig. 2.

As shown in Fig. 4(a), for the lowest parallel pressures ($P^*_{//} = 0.25$ and 0.5), the average density of the simulated systems tends to increase relatively to the corresponding bulk values (about 180% in the extreme case) when pore width is

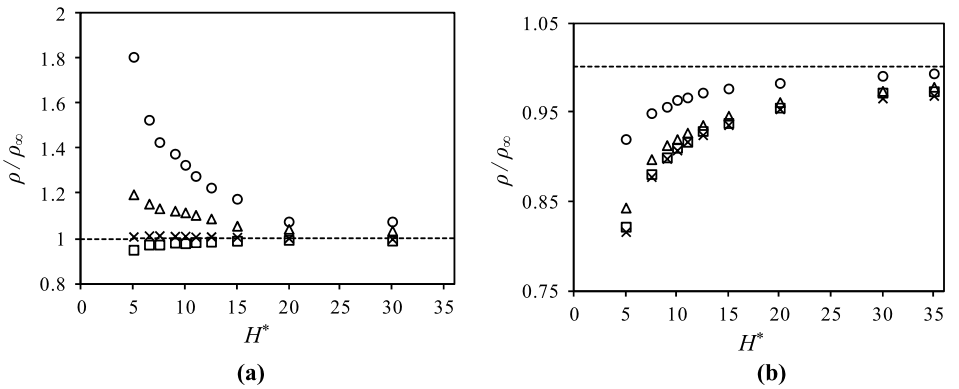


**Fig. 4.** Average density relatively to the bulk value for atomistic (a) and structureless (b) walls as a function of pore widths, for $P^*_{//} = 0.25$ (circles), $P^*_{//} = 0.5$ (triangles), $P^*_{//} = 0.75$ (across) and $P^*_{//} = 1$ (squares).

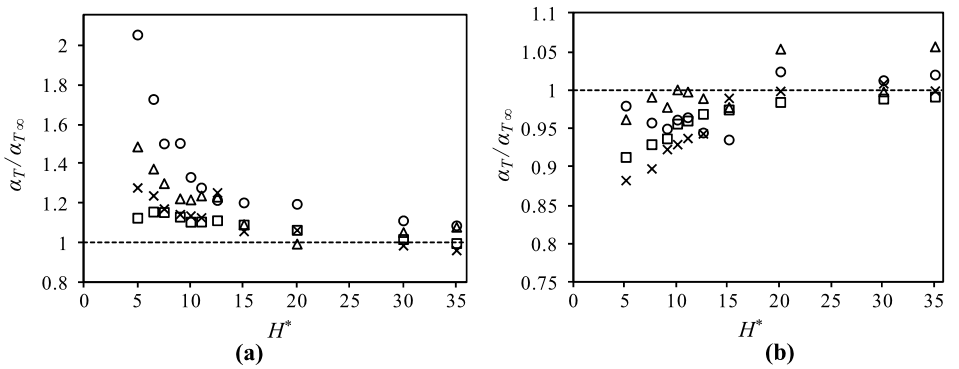


**Fig. 5.** Thermodiffusion factor relatively to the bulk value for atomistic (a) and structureless (b) walls as a function of pore widths, $P^*_{//} = 0.25$ (circles), $P^*_{//} = 0.5$ (triangles), $P^*_{//} = 0.75$ (across) and $P^*_{//} = 1$ (squares).

decreasing, as expected from the local density profiles shown in Fig. 2(a). Furthermore, this increase is more pronounced for $P^*_{//} = 0.25$ than for $P^*_{//} = 0.5$. For $P^*_{//} = 0.75$, the average density is almost the same for all pore widths and is equal to that of bulk fluid. Finally, for $P^*_{//} = 1$, the average density tends to weakly decrease with pore width (5% at most), consistently with what shown in Fig. 2(b). In Fig. 4(b), density tends to decrease when pore width decreases (up to 18% in the extreme case) for all parallel pressures tested. Furthermore, for the lowest parallel pressure, the decrease is less pronounced than for the others parallel pressures tested, which exhibit almost the same behaviour with pore widths.

From these results, we can confirm, as already shown in Fig. 2, that the structureless pore (LJ 9–3) is not able to yield results similar to that of a fully atomistic pore, especially at low pressure and in very narrow pores. From this, we can expect that the transport properties will as well be influenced by the choice of the nature of the description of the walls.

### *3.2. Thermodiffusion*

For the systems described in the previous section, NEMD simulations have been performed to estimate the thermodiffusion factors of the studied binary mixture. For that purpose, we used the linear parts of the molar fraction gradient of the heavy component and of the temperature profiles in the *x*-direction. To quantify the porous medium effect, we have compared the results in the confined situations with the thermodiffusion in bulk fluid for the same thermodynamic conditions. For the bulk fluid we have obtained $\alpha_T = 0.47 \pm 0.05$, $0.86 \pm 0.005$, $1.22 \pm 0.09$ and $1.44 \pm 0.11$ for $P^*_{//} = 0.25$, 0.5, 0.75 and 1, respectively. These results are in agreement with those of Ref. [20].

Fig. 5 shows that there is an opposite effect of the pore width on $\alpha_T$ in atomistic and structureless walls. The thermodiffusion factor tends to decrease in structureless walls when the pore width is decreasing while it is the contrary for the atomistic walls. Additionally, we can note a weak effect of the confinement in structureless walls, which is at most of the order of the error bars. However, in atomistic walls, the thermodiffusion factor is strongly affected (up to 200% in extreme case), and is more pronounced when the parallel pressure is decreasing. It should be pointed out that, as expected, for all cases the thermodiffusion factor tends toward the bulk values when the pore width is increasing.

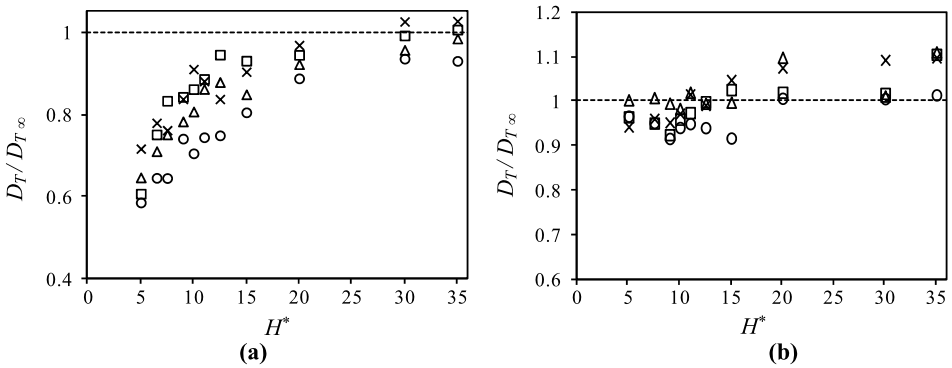


**Fig. 6.** Thermodiffusion coefficient relatively to the bulk value for atomistic (a) and structureless (b) walls as a function of pore widths, for $P^*_{//} = 0.25$ (circles), $P^*_{//} = 0.5$ (triangles), $P^*_{//} = 0.75$ (across) and $P^*_{//} = 1$ (squares).

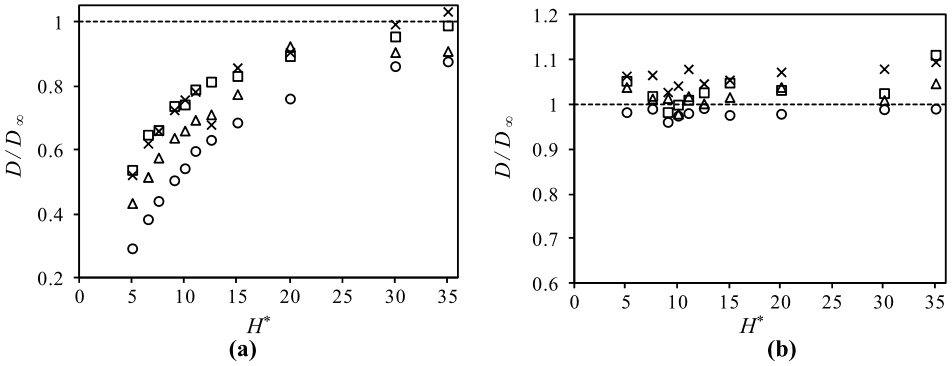


**Fig. 7.** Mass diffusion coefficient relatively to the bulk value for atomistic (a) and structureless (b) walls as a function of pore widths, for $P^*_{//} = 0.25$ (circles), $P^*_{//} = 0.5$ (triangles), $P^*_{//} = 0.75$ (across) and $P^*_{//} = 1$ (squares).

In bulk fluids, $\alpha_T$ is increasing with density for such states [20]. Thus, putting aside the fact that the surface of the two wall types are different, it seems that the results obtained here in confined situations are consistent with the density results when looking at Figs. 4 and 5. However, to better understand these trends and in particular the impact of the roughness of the walls, we have evaluated the effect of confinement on mass diffusion and thermodiffusion coefficients in the next section.

### 3.3. Mass diffusion and thermodiffusion coefficients

To supplement the previous results, we have evaluated the thermodiffusion coefficients for the same systems in the same thermodynamics conditions. To do so, the mass diffusion coefficient has been computed and the thermodiffusion coefficient deduced from Eq. (5). The results are shown in Fig. 6.

Fig. 6(a) shows that, contrary to the thermodiffusion factor, the thermodiffusion coefficient of a fluid confined between atomistic walls tends to decrease when the pore width is decreasing for all parallel pressures tested. Those results are completely different from that obtained with structureless wall (Fig. 6(b)), where we can observe a weak effect of the confinement on $D_T$. To understand these surprising trends, we have plotted the results for the mass diffusion coefficient in Fig. 7. To quantify the porous medium effect we also have computed mass diffusion coefficient in bulk fluid and we have obtained $D^*_\infty = 19.84 \pm 0.20$, $8.90 \pm 0.09$, $5.96 \pm 0.06$ and $4.91 \pm 0.04$ for $P^*_{//} = 0.25$, 0.5, 0.75 and 1, results in agreement with [21].

Fig. 7(a) shows a strong dependence of the mass diffusion coefficient on the confinement in atomistic walls. In all cases, the mass diffusion coefficient decreases with the pore width in a similar fashion for all pressures (more pronounced when the pressure decreases). These trends are completely different in structureless walls (Fig. 7(b)), where we can observe a weak effect of confinement on mass diffusion. Interestingly, these two behaviours cannot be explained by average density effects (Fig. 4) as long as $D$ is decreasing when density increases.

In fact, these trends can be explained, for both thermodiffusion and mass coefficients, by taking into account the fact that the boundary conditions on the fluid due to atomistic walls and structureless walls are completely different. For the first wall type (atomistic), because of the roughness, the slip of the fluid on the walls is very limited, while this slip is non-negligible when using structureless (flat) walls. This has been confirmed using molecular dynamics simulations by Saugey

and co-workers [14]. They showed that the mass diffusion coefficient is very sensitive to boundary conditions on the solid substrate. Furthermore, because of adsorption, the local mass diffusion close to an atomistic wall is reduced compared to that of the bulk [22].

As thermodiffusion coefficient in such an isotopic mixture is a purely kinetic property (the potential of the two compounds is exactly the same), such explanations for the mass diffusion coefficient should hold as well for the thermodiffusion coefficient. Thus, in this case, the difference of friction on the solid due to the wall roughness seems to be the dominant effect to explain the noticed behaviour on mass and thermodiffusion coefficients.

## 4. Conclusion

To summarize, we have studied in this paper the effect of corrugation (structureless and atomistic walls), parallel pressure and pore width on thermodiffusion and mass diffusion in simple isotopic mixture confined in a slit pore. To do so, we have performed non-equilibrium molecular dynamics (NEMD) simulations of Lennard–Jones binary equimolar mixtures confined in atomistic and structureless walls with various widths (5 to 35 times the size of a molecule), at four different parallel pressures in super-critical conditions. To do so, a new algorithm has been developed to control the parallel pressure.

It has been found that the roughness of the wall has a large impact on the thermal diffusion factor's dependence with the pore width. This dependence is in fact strongly related to the behaviour of the average density with the pore width, which noticeably differs between the two wall types because of differences between effective fluid–solid interactions. More precisely, in an atomistic wall the thermal diffusion factor tends to increase strongly when the pore width is decreasing, and this dependence increases when parallel pressure is decreasing. However, in a structureless wall this effect can be considered as negligible for the pore widths larger than 10 times the size of the molecules and whatever the parallel pressure used, consistently with previous findings.

When looking at the mass diffusion and thermodiffusion coefficients separately, it has been shown that both quantities are largely influenced by pore size in an atomistic wall (a strong decrease when the pore width decreases), whereas it is not the case when using structureless walls. For both mass and thermodiffusion diffusion coefficients, these trends can be explained by taking into account the fact that the boundary conditions on the fluid due to atomistic walls (friction) and structureless walls (slip) are completely different.

## Acknowledgements

We gratefully acknowledge computational facilities provided by the UPPA, by the I2M and the MCIA in Bordeaux (supported by the Region Aquitaine). R.H. acknowledges the French Ministry of Research for the grant provided to perform this work. This work has been partially supported by TOTAL in the frame of a Tight Gas Reservoir project and by an ERC advanced grant under the “Failflow” project.

## References

[1] S.R. de Groot, P. Mazur, Non-Equilibrium Thermodynamics, Dover Publications Inc., New York, 1984.
[2] C. Lira-Galeana, A. Firoozabadi, J.M. Prausnitz, Computation of compositional grading in hydrocarbon reservoirs application of continuous thermodynamics, Fluid Phase Equilibria 102 (1994) 143–158.
[3] F. Montel, J. Bickert, A. Lagisquet, G. Galliéro, Initial state of petroleum reservoirs: A comprehensive approach, Journal of Petroleum Science and Engineering 58 (2007) 391–402.
[4] M. Touzet, G. Galliéro, V. Lazzeri, M.Z. Saghir, F. Montel, J.-C. Legros, Thermodiffusion: from microgravity experiments to the initial state of petroleum reservoirs, Comptes Rendus Mécanique 339 (2011) 318–323.
[5] A.A. Shapiro, E.H. Stenby, Factorization of transport coefficients in macroporous media, Transport in Porous Media 41 (2000) 305–323.
[6] J.K. Platten, P. Costesèque, The soret coefficient in porous media, Journal of Porous Media 7 (2004) 317–329.
[7] M. Schoen, Computer Simulation of Condensed Phases in Complex Geometries, Springer-Verlag, Berlin, Heidelberg, 1993.
[8] I. Wold, B. Hafskjold, Nonequilibrium molecular dynamics simulations of coupled heat and mass transport in binary fluid mixtures in pores, International Journal of Thermophysics 20 (1999) 847–856.
[9] J. Colombani, G. Galliéro, B. Duguay, J.-P. Caltagirone, F. Montel, P.A. Bopp, A molecular dynamics study of thermal diffusion in a porous medium, Physical Chemistry Chemical Physics 4 (2002) 313–321.
[10] J. Colombani, G. Galliéro, B. Duguay, J.-P. Caltagirone, F. Montel, P.A. Bopp, Molecular dynamics study of thermal diffusion in a binary mixture of alkanes trapped in a slit pore, Philosophical Magazine 83 (2003) 2087–2095.
[11] G. Galliéro, J. Colombani, P.A. Bopp, J.-P. Caltagirone, F. Montel, Thermal diffusion in micropores by molecular dynamics computer simulation, Physica A: Statistical Mechanics and its Applications 361 (2006) 494–510.
[12] S. Yeganegi, E. Pak, The effect of corrugation of pore wall on the thermal diffusion in nanopores by molecular dynamics simulations, Chemical Physics 333 (2007) 69–76.
[13] R. Hannaoui, G. Galliéro, D. Ameur, C. Boned, Molecular dynamics simulations of heat and mass transport properties of a simple binary mixture in micro/meso-pores, Chemical Physics 389 (2011) 53–57.
[14] A. Saugey, L. Joly, C. Ybert, J.-L. Barrat, L. Bocquet, Diffusion in pores and its dependence on boundary conditions, Journal of Physics Condensed Matter 17 (2005) S4075–S4090.
[15] J.C. Wang, K.A. Fichthorn, A method for molecular dynamics simulation of confined fluids, Journal of Chemical Physics 112 (2000) 8252–8259.
[16] M.P. Allen, D.J. Tildesley, Computer Simulation of Liquids, Clarendon Press, Oxford, UK, 1987.
[17] H. Eslami, F. Mozaffari, J. Moghadasi, F. Müller-Plathe, Molecular dynamics simulation of confined fluids in isosurface-isothermal-isobaric ensemble, Journal of Chemical Physics 129 (2008) 194702.
[18] H.J.C. Berendsen, J.P.M. Postma, W.F. van Gunsteren, A. DiNola, J.R. Haak, Molecular dynamics with coupling to an external bath, Journal of Chemical Physics 81 (1984) 3684–3690.

[19] F. Müller-Plathe, D. Reith, Cause and effect reversed in non-equilibrium molecular dynamics: an easy route to transport coefficients, Computational and Theoretical Polymer Science 9 (1999) 203–209.
[20] G. Galliéro, M. Bugel, B. Duguay, F. Montel, Mass effect on thermodiffusion using molecular dynamics, Journal of Non-Equilibrium Thermodynamics 32 (2007) 251–258.
[21] M.S. Zabaloy, V.R. Vasquez, E.A. Macedo, Description of self-diffusion coefficients of gases, liquids and fluids at high pressure based on molecular simulation data, Fluid Phase Equilibria 242 (2006) 43–56.
[22] H. Hoang, G. Galliero, Grand canonical-like molecular dynamics simulations: Application to anisotropic mass diffusion in a nanoporous medium, Journal of Chemical Physics 136 (2012) 184702.